6th Intercontinental Geoinformation Days

igd.mersin.edu.tr

Using frequency ratio model for flood susceptibility mapping of Mandaue City, Cebu

Jao Hallen Bañados *[1], **Isabella Pauline Quijano**[1], **Chito Patiño**[1]

[1]*University of the Philippines Cebu, SMART-TUrF, College of Science, Cebu City, Philippines*

Keywords
Flood susceptibility
Frequency ratio
GIS
ROC

Abstract

Floods cause damage to the global economy and environment, leading to the loss of lives; therefore, identifying flood-vulnerable locations is essential for complete flood risk management. As a highly dense and low-lying city, Mandaue City in Cebu, Philippines, easily gets flooded during heavy downpours leading to heavy traffic and damages in the area. This study utilized a geospatial approach to generate a flood susceptibility map of the city using the frequency ratio (FR) model. The flood susceptibility analysis considered eight flood conditioning factors: elevation, slope, Topographic Wetness Index (TWI), curvature, river density, land use, Normalized Difference Vegetation Index (NDVI), and rainfall. The FR model results exhibited high accuracy, with an AUC value of 0.902. Five percent of the city falls under high hazard classification, encompassing industrial, commercial, and critical facilities.

1. Introduction

Rapid urbanization and climate change have resulted in numerous environmental issues and tragedies (Rahmati et aal. 2019). The Philippines experiences around 20 tropical cyclones annually, with the peak season occurring from July to October, accounting for about 70% of all typhoons (Santos 2020).

Mandaue City is prone to flooding during heavy downpours, causing traffic congestion and damage. Hence, flood prevention is crucial to protect livelihoods and the environment (Huang et al. 2008). Geographic information systems (GIS) and remote sensing have been used in various studies to analyze flood hazards and map flood susceptibility (Bates 2004; Paul et al. 2019; Rahmati et al. 2016; Yariyan et al. 2020). Accurate identification of flood-prone areas is essential for effective flood management and prevention (Termeh et al. 2018). Flood susceptibility modeling, incorporating GIS and remote sensing, helps identify vulnerable areas (Wang 2019). Flood inventory maps serve as primary data sources for flood susceptibility mapping, and techniques like logistic regression and frequency ratio (FR) models are used to assess flood risk (Ullah et al. 2020). The FR model, known for its simplicity and satisfactory risk analysis, was chosen for this study (Ullah et al. 2020). Although not commonly used for flood hazards, the FR model has shown promising results for other natural hazards like landslides (Nicu 2017; Aditian et al. 2018; Regmi et al. 2014)

The study's main objective is to generate a flood susceptibility map of Mandaue City, focusing on the Butuanon river basin, using the FR model and identify potential flood risk areas within the city.

2. Method

2.1. Description of study area

Mandaue City, located in the province of Cebu in the Philippines, is a commercial and industrialized urban area situated at coordinates 10.3321° N and 123.9357° E. It is a high-income city and is surrounded by other highly-urbanized cities, as shown in Figure 1. The climate in the region follows a wet and dry season pattern, with the rainy season lasting from June to November, classified as Coronas climate type 3. The city receives an average annual precipitation of 1,570 millimeters (JICA 2010).

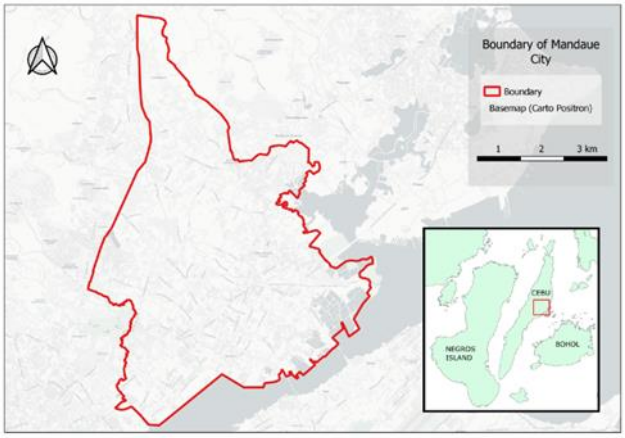

Figure 1. Mandaue City, Cebu, Philippines

* **Corresponding Author**

*(jlbanados@up.edu.ph) ORCID ID 0000-0002-7675-1762
(ilquijano@up.edu.ph) ORCID ID 0000-0002-7579-7267
(clpatino@up.edu.ph) ORCID ID 0000-0001-6879-2268

Cite this study

Bañados, J. H., Quijano, I. P., Patiño, C. (2023). Using frequency ratio model for flood susceptibility mapping of Mandaue City, Cebu. Intercontinental Geoinformation Days (IGD), 6, 78-82, Baku, Azerbijan

2.2. Flood inventory mapping

The accuracy of flood susceptibility mapping relies on accurate historical flood data (Ullah et al. 2020). In this study, flood-prone areas were identified based on the city's 2020 Comprehensive Drainage Master Plan and Drainage Impact Assessment. 163 flood points were recognized and categorized in the flood inventory database with input from residents.

2.3. Flood conditioning factors

Flood susceptibility assessment requires considering multiple flood-triggering and causing factors and their relationship to flooding. The selection of flood-controlling factors is not standardized and varies across studies (Samanta et al. 2018; Das 2019; Dou et al. 2018). In this study, flood conditioning factors were chosen based on the physical and natural characteristics of the study area and data availability. The flood conditioning parameters included elevation, slope, Topographic Wetness Index (TWI), river density, land use, rainfall, Normalized Difference Vegetation Index (NDVI), and curvature.

The Interferometric Synthetic Aperture Radar (IFSAR) Digital Elevation Model (DEM) was utilized to generate the elevation, slope, TWI, and curvature rasters. Land use and river density datasets were extracted by the City Planning Division of the city. The NDVI and rainfall datasets were obtained using the Google Earth Engine platform. The NDVI raster was specifically acquired using the Landsat-8 images collection, which covers the 2013-2022 dataset. Meanwhile, the rainfall raster was extracted from Climate Hazards Group InfraRed Precipitation with Station Data (CHIRPS). All factors were then reclassified into six classes using the natural break classification, except for the curvature raster (Pawar et al. 2022).

2.4. Frequency ratio (FR) model

Frequency ratio is an extensively used model in the analysis and mapping of different types of natural hazards, including floods, landslides, and forest fires (Rehman et al. 2022). Each independent flood triggering factor's relationship to the likelihood of flooding determined its measure of probability. The link between flood incidence and flood-triggering factors is strongest when the probability is larger (greater than 1) and weakest when the probability is lower (less than 1) (Samanta et al. 2018). The FR formula is expressed in Equation 1:

$$FR = \frac{Flood\ Points\ per\ Factor\ Class\ /\ Total\ Flood\ Points\ per\ Factor\ Class}{Area\ per\ Factor\ Class/\ Total\ Area} \quad (1)$$

The results were then normalized as relative frequency (RF) into a range of probability values [0, 1]. Even after normalization, the RF still has the flaw of assigning equal weight to each contributing factor. A prediction rate (PR) was produced by grading each flood conditioning factor with the training data set to solve this issue. Finally, the flood susceptibility map can be generated using the summation of the PR of each factor and the RF of each class using the Equation 2.

$$FS = \sum_{i=1}^{n} PR_i \times RF_i \quad (2)$$

3. Results

The FR model was used to assess Mandaue City's flood susceptibility by analyzing the relationship between flood-prone areas and flood conditioning factors. Table 1 presents the reclassification results and occurrences of each factor related to flood hazards.

Low-lying areas, accounting for 38.15% of the city, had a high RF value (0.304) and were prone to flooding. Nearly 92% of past floods occurred in the first three elevation classes are consistent with previous research (Khosravi et al. 2019). Low-gradient slopes in lower regions were found to be more susceptible to flooding compared to high-gradient slopes (Ramesh et al. 2020). The lowest slope gradient class (<1.838°) covered 70.36% of the study area and had a high occurrence of past floods (74.58%). The TWI factor in this study was categorized into five classes. Flood occurrences were lower in the last TWI class, while classes ranging from 5.903 to 9.2 had a higher susceptibility to flooding. Reclassification results revealed that higher TWI values were predominantly found in streams and low-lying areas, while the uplands had lower TWI values. Flooding in the watershed was more likely in areas with higher TWI values (Tehrany et al. 2015).

Drainage density plays a critical role in flooding, as higher density indicates increased surface runoff and a greater likelihood of flooding (Ullah et al. 2020) The study found that the highest drainage density was near the Butuanon River, which is located in the middle of the city and is a major contributor to flooding (Maglana et al. 2020). The occurrence of flooding was most likely in areas classified in the third to fifth classes, with a probability of 70.08%. Regions with high drainage density have a higher risk of flooding due to increased surface runoff (Das 2019). Land use patterns reflect how the city utilizes its land. In terms of flooding, built-up areas contribute to increased runoff due to extensive impermeable surfaces and a lack of vegetation to slow down or absorb water. Barren ground also enhances runoff. In this study, higher weights were assigned to waterbodies (RF of 0.285) and mangrove forest areas (RF of 0.329). Built-up areas near rivers, with their economic resources, infrastructure, and large population, are particularly susceptible to flooding (Khosravi et al. 2016). Positive NDVI values indicate vegetation, while negative values represent water. Therefore, higher NDVI levels suggest a lower risk of flooding, while lower NDVI values indicate a higher potential for flooding (Khosravi et al. 2016). For the NDVI of the area, values range from -0.224 to 0.745. The curvature analysis, derived from the same DEM as elevation and slope, represented the topography's morphology. It was divided into three classes: convex, flat, and concave. Positive curvature values indicated convex surfaces, zero represented flat surfaces, and negative values indicated concave surfaces. The study found that the majority of the study area

belonged to the middle class, which had relatively flat topography and accounted for 93.47% of flood occurrences.

Table 1. Flood conditioning factors and classes

Factor	Class	Occurrence	%
Elevation (m)	0-7.61	23278	54.65
	7.61-17.26	5424	12.73
	17.26-29.95	10516	24.69
	29.95-49.25	2022	4.75
	49.25-77.17	956	2.24
	77.17-129.97	398	0.93
Slope (degree)	0-1.84	31881	74.85
	1.84-5.18	6363	14.94
	5.18-10.03	2348	5.51
	10.03-16.38	1143	2.68
	16.38-23.9	509	1.2
	23.9-42.78	350	0.82
TWI	2.52-5.9	4783	11.23
	5.9-7.64	11922	27.99
	7.64-9.2	11724	27.53
	9.2-10.85	8376	19.66
	10.85-13.36	4402	10.33
	13.36-24.72	1387	3.26
Drainage	0-0.76	490	10.47
Density	0.76-2.01	425	9.08
	2.01-3.16	1042	22.26
	3.16-4.31	1116	23.84
	4.31-5.71	1123	23.99
	5.71-9.2	486	10.38
Land Use	Brush/Shrubs	138	2.32
	Built-up	4432	74.59
	Inland Water	970	16.32
	Mangrove Forest	97	1.63
	Open/Barren	293	4.93
	Perennial Crop	12	0.2
Rainfall (mm)	53.54-56.38	655	14.15
	56.38-61.15	26	0.56
	61.15-66.94	3471	75
	66.94-72.42	6	0.13
	72.42-76.48	127	2.74
	76.48-79.52	343	7.41
NDVI	-0.22-0.06	559	12.1
	0.06-0.14	1013	21.94
	0.14-0.23	1068	23.13
	0.23-0.32	910	19.71
	0.32-0.44	686	14.85
	0.44-0.75	382	8.27
Curvature	-12.47--1.31	809	1.9
	-1.31-0.56	39813	93.47
	0.56-12.81	1972	4.63

4. Discussion

To create the final flood susceptibility map, the weights of each factor and the RF of each class were summed using the flood susceptibility index equation in the ArcGIS 10.8 environment (Samanta et al. 2018). The resulting raster was divided into four classes, with only three classes representing hazard levels: low, moderate, and high, as shown in Figure 2. The analysis reveals that approximately 5% of the total area is in a high-hazard zone, 27% in a moderate zone, and 36% in a low-hazard zone. The remaining 32% of the city is considered safe, as summarized in Table 2.

Table 2. Hazard classes

Hazard Class	Class Area (sq. m)	% of Area
Very Low	10719	32
Low	12076	36
Moderate	9242	27
High	1634	5

Figure 2 illustrates that the high-risk areas for flooding are primarily located near the banks and mouth of rivers and streams, particularly along the Butuanon River. Upon examining the intersection of flood susceptibility and the buildings dataset, it becomes evident that numerous residential areas, commercial buildings, industrial zones, and critical facilities are highly vulnerable to future flooding.

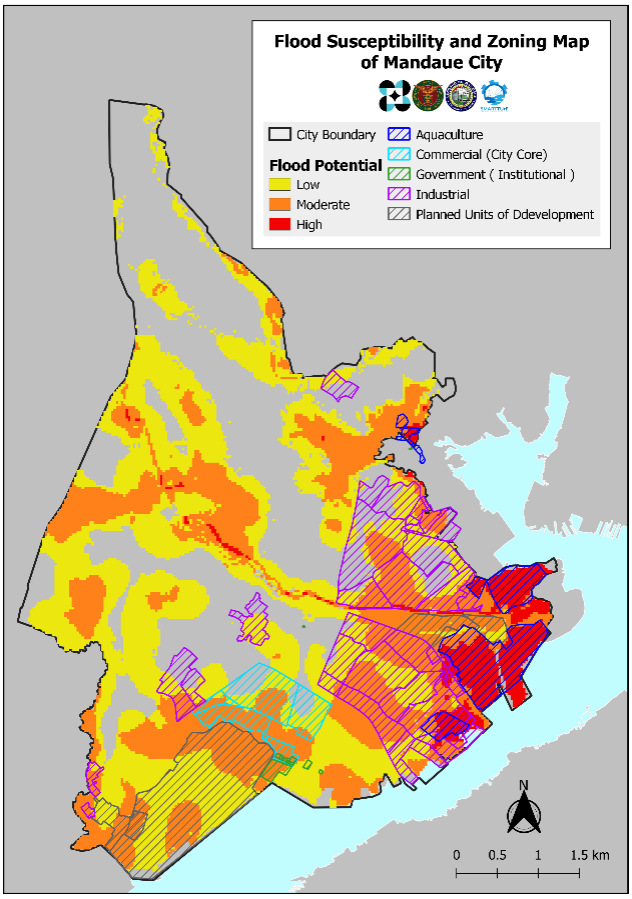

Figure 2. Flood susceptibility map and zoning map of Mandaue City

5. Conclusion

Floods are a significant global environmental hazard, causing widespread devastation. To mitigate the impact of floods, it is essential to assess flood vulnerability and generate flood susceptibility maps. This study utilized a

GIS-based approach with the frequency ratio method to create a flood susceptibility map of Mandaue City. Eight flood conditioning factors, including elevation, slope, TWI, river density, land use, rainfall, NDVI, and curvature, were analyzed. The effectiveness of the frequency ratio model was evaluated using the ROC curve, resulting in a success rate of 90.2% as depicted in Figure 3. The flood conditioning factors played a crucial role in mapping flood vulnerability.

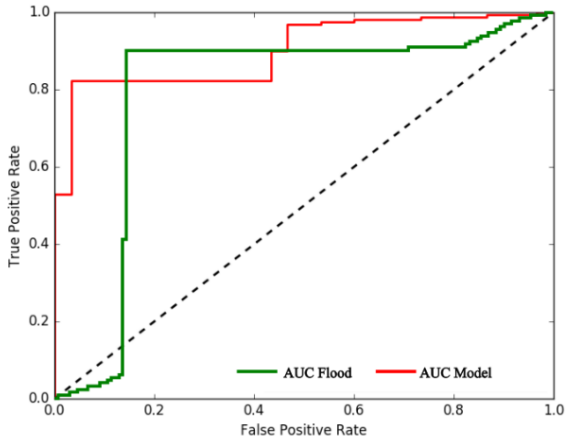

Figure 3. AUC graph of the FR model and flood hazard

Acknowledgement

This research was conducted by the Smart City Solutions to Urban Flooding Program. We are grateful to the Department of Science and Technology (DOST) for the financial support, with the DOST Philippine Council for Industry, Energy, and Emerging Technology Research and Development as the monitoring agency and the University of the Philippines Cebu as the implementing agency.

References

Aditian, A., Kubota, T., & Shinohara, Y. (2018). Comparison of GIS-based landslide susceptibility models using frequency ratio, logistic regression, and artificial neural network in a tertiary region of Ambon, Indonesia. Geomorphology, 318, 101-111.

Bates, P. D. (2004). Remote sensing and flood inundation modelling. Hydrological processes, 18(13), 2593-2597.

Das, S. (2019). Geospatial mapping of flood susceptibility and hydro-geomorphic response to the floods in Ulhas basin, India. Remote Sensing Applications: Society and Environment, 14, 60-74.

Debabrata, S., & Mondal, P. (2020). Flood vulnerability mapping using frequency ratio (FR) model: a case study on Kulik river basin, Indo-Bangladesh Barind region. Applied Water Science, 10(17).

Dou, X., Song, J., Wang, L., Tang, B., Xu, S., Kong, F., & Jiang, X. (2018). Flood risk assessment and mapping based on a modified multi-parameter flood hazard index model in the Guanzhong Urban Area, China. Stochastic environmental research and risk assessment, 32, 1131-1146.

Huang, X., Tan, H., Zhou, J., Yang, T., Benjamin, A., Wen, S. W., ... & Li, X. (2008). Flood hazard in Hunan province of China: an economic loss analysis. Natural Hazards, 47, 65-73.

Japan International Cooperation Agency (JICA). (2010).

Khosravi, K., Pourghasemi, H. R., Chapi, K., & Bahri, M. (2016). Flash flood susceptibility analysis and its mapping using different bivariate models in Iran: a comparison between Shannon's entropy, statistical index, and weighting factor models. Environmental monitoring and assessment, 188, 1-21.

Khosravi, K., Melesse, A. M., Shahabi, H., Shirzadi, A., Chapi, K., & Hong, H. (2019). Flood susceptibility mapping at Ningdu catchment, China using bivariate and data mining techniques. In Extreme hydrology and climate variability (pp. 419-434). Elsevier.

Maglana, J. M. R., Parmes, H. O. O., Yu, A. C. C., Fornis, R. L., & Oraya, A. F. A. (2020, October). An attempt to classify landcover of the Butuanon river catchment using Landsat images covering the years 1993 to 2019 for rainfall-runoff modelling. In AIP Conference Proceedings (Vol. 2278, No. 1). AIP Publishing.

Nicu, I. C. (2017). Frequency ratio and GIS-based evaluation of landslide susceptibility applied to cultural heritage assessment. Journal of Cultural Heritage, 28, 172-176.

Paul, G. C., Saha, S., & Hembram, T. K. (2019). Application of the GIS-based probabilistic models for mapping the flood susceptibility in Bansloi sub-basin of Ganga-Bhagirathi river and their comparison. Remote Sensing in Earth Systems Sciences, 2, 120-146.

Pawar, U., Suppawimut, W., Mutiil, N., & Rathnayake, U. (2022). A GIS-Based Comparative Analysis of Frequency Ratio and Statistical Index Models for Flood Susceptibility Mapping in the Upper Krishna Basin, India. Water, 14, 3771.

Rahmati, O., Zeinivand, H., & Besharat, M. (2016). Flood hazard zoning in Yasooj region, Iran, using GIS and multi-criteria decision analysis. Geomatics, Natural Hazards and Risk, 7(3), 1000-1017.

Rahmati, O., Darabi, H., Haghighi, A. T., Stefanidis, S., Kornejady, A., Nalivan, O. A., & Tien Bui, D. (2019). Urban flood hazard modeling using self-organizing map neural network. Water, 11(11), 2370.

Ramesh, V., & Iqbal, S. S. (2020). Urban flood susceptibility zonation mapping using evidential belief function, frequency ratio and fuzzy gamma operator models in GIS: a case study of Greater Mumbai, Maharashtra, India. Geocarto International.

Regmi, A. D., Yoshida, K., Pourghasemi, H. R., Dhital, M. R., & Pradhan, B. (2014). Landslide susceptibility mapping along Bhalubang—Shiwapur area of mid-Western Nepal using frequency ratio and conditional probability models. Journal of Mountain Science, 11, 1266-1285.

Rehman, A., Song, J., Haq, F., Mahmood, S., Ahamad, M. I., Basharat, M., ... & Mehmood, M. S. (2022). Multi-hazard susceptibility assessment using the analytical hierarchy process and frequency ratio techniques in the Northwest Himalayas, Pakistan. Remote Sensing, 14(3), 554.

Samanta, R. K., Bhunia, G. S., Shit, P. K., & Pourghasemi, H. R. (2018). Flood susceptibility mapping using geospatial frequency ratio technique: a case study of

Subarnarekha River Basin, India. Modeling Earth Systems and Environment, 4, 395-408.

Santos, G. D. (2021). 2020 Tropical Cyclones in the Philippines: A Review. Tropical Cyclone Research and Review, 10(3), 191-199.

Tehrany, M. S., Pradhan, B., Mansor, S., & Ahmad, N. (2015). Flood susceptibility assessment using GIS-based support vector machine model with different kernel types. Catena, 125, 91-101.

Termeh, S. V. R., Kornejady, A., Pourghasemi, H. R., & Keesstra, S. (2018). Flood susceptibility mapping using novel ensembles of adaptive neuro-fuzzy inference system and metaheuristic algorithm. Sci. Total Environ., 615, 438-451.

Ullah, K., & Zhang, J. (2020). GIS-based flood hazard mapping using relative frequency ratio method: A case study of Panjkora River Basin, Eastern Hindu Kush, Pakistan. PLoS ONE, 15(3), e0229153.

Wang, Y. (2019). Flood susceptibility mapping in Dingnan County (China) using adaptive neuro-fuzzy inference system with biogeography-based optimization and imperialistic competitive algorithm. Journal of Environmental Management, 247, 712-729.

Yariyan, P., Avand, M., Abbaspour, R. A., Torabi Haghighi, A., Costache, R., Ghorbanzadeh, O., ... & Blaschke, T. (2020). Flood susceptibility mapping using an improved analytic network process with statistical models. Geomatics, Natural Hazards and Risk, 11(1), 2282-2314.